TaXa21, a Leucine-Rich Repeat Receptor–Like Kinase Gene Associated with *TaWRKY76* and *TaWRKY62*, Plays Positive Roles in Wheat High-Temperature Seedling Plant Resistance to *Puccinia striiformis* f. sp. *tritici*

Jiahui Wang,[1] Junjuan Wang,[1] Hongsheng Shang,[1] Xianming Chen,[2] Xiangming Xu,[3] and Xiaoping Hu[1,†]

[1] State Key Laboratory of Crop Stress Biology for Arid Areas and College of Plant Protection, Northwest A&F University, Taicheng Road 3, Yangling, Shaanxi 712100, China
[2] Agricultural Research Service, United States Department of Agriculture and Department of Plant Pathology, Washington State University, Pullman, WA 99164-6430, U.S.A.
[3] NIAB East Malling Research, New Road, East Malling, ME19 6BJ, Kent, U.K.

Puccinia striiformis f. sp. *tritici* causes wheat stripe rust, one of most important diseases of wheat worldwide. High-temperature seedling plant (HTSP) resistance of wheat to *P. striiformis* f. sp. *tritici* is one specific type of host resistance, induced by high temperature (HT). Receptor-like kinases (RLKs) play key roles in regulating plant development and signaling networks, but there have been no reports on possible roles played by RLKs in wheat HTSP to *P. striiformis* f. sp. *tritici*. In the present study, a leucine rich repeat (LRR)-RLK gene, *TaXa21*, with a high homology with rice bacterial blight resistance gene *Xa21*, was cloned from wheat cultivar Xiaoyan 6 (XY 6). *TaXa21* expression was up-regulated by the exposure to HT (20°C) for 24 h at 8 days postinoculation with *P. striiformis* f. sp. *tritici* and was induced by ethylene (ET) and hydrogen peroxide (H_2O_2). Knocking down *TaXa21* using virus-induced gene silencing reduced HTSP resistance to *P. striiformis* f. sp. *tritici* compared with the control plants. In addition, the expression level of *TaCAT* in the H_2O_2 pathway was induced and *TaACO* in the ET signal pathway was reduced in the HT-treated *TaXa21*-silenced plants. Transient expression of *TaXa21* in tobacco leaves confirmed its subcellular localization in plasma membrane, consistent with the prediction from bioinformatics analysis. The transmembrane and kinase domain of TaXa21 can interact with TaWRKY76 in the nucleus and cell membrane, which is different from the localization of Xa21 in rice. The interaction between TaWRKY76 and TaWRKY62 (positively involved in the HTSP resistance of XY 6) were observed. Together, these results indicated that *TaXa21* is a RLK associated with *TaWRKY76* and *TaWRKY62* and functions as a positive regulator of wheat HTSP resistance to *P. striiformis* f. sp. *tritici*. Furthermore, the host defense is mediated by the H_2O_2 and ET signal pathways.

Keywords: high-temperature seedling plant resistance, stripe rust, *TaXa21*, *TaWRKY76*, *TaWRKY62*, interaction

Stripe rust, caused by *Puccinia striiformis* f. sp. *tritici*, is one of the most devastating fungal diseases of wheat worldwide (Chen 2005). Breeding resistant cultivars is the most cost-effective and environment-friendly approach to control *P. striiformis* f. sp. *tritici* (Chen 2007; Chen and Line 1995; Sui et al. 2009; Zhang et al. 2001). However, wheat resistance to *P. striiformis* f. sp. *tritici* is frequently overcome by the pathogen (Peng et al. 1999).

High-temperature (HT) resistance of wheat to *P. striiformis* f. sp. *tritici* is induced by exposure of wheat plants to HT. Based on the growth stage, HT resistance can be divided into two types, high-temperature seedling plant (HTSP) resistance and high-temperature adult-plant (HTAP) resistance (Chen 2013). Wheat plants with HTAP resistance are susceptible to *P. striiformis* f. sp. *tritici* in the seedling stage but become resistant in the adult stage under HT (Chen et al. 2013). In contrast, the HTSP resistance is expressed throughout the entire wheat growth period when seedlings were exposed to 20°C only for 24 h during the initial *P. striiformis* f. sp. *tritici* incubation stage (Ma and Shang 2000; Tao et al. 2018). Compared with the HTAP resistance to *P. striiformis* f. sp. *tritici*, there have been fewer studies on the mechanisms of the HTSP resistance to *P. striiformis* f. sp. *tritici*. Xiaoyan 6 (XY 6) is a wheat cultivar exhibiting the typical HTSP resistance to *P. striiformis* f. sp. *tritici*; XY 6 has maintained the HTSP resistance against *P. striiformis* f. sp. *tritici* under field conditions for more than 30 years (Ma and Shang 2000) and is still grown commercially in China.

Receptor-like kinases (RLKs), one of the largest protein families, with at least 600 members, can induce pathogen-associated molecular pattern (PAMP)-triggered immunity (PTI) or effector-triggered immunity (ETI) plant defense responses against pathogens (Shiu and Bleecker 2001). A typical RLK

[†]Corresponding author: X. Hu; xphu@nwsuaf.edu.cn

*The *e*-Xtra logo stands for "electronic extra" and indicates that two supplementary figures and one supplementary table are published online.

The author(s) declare no conflict of interest.

contains a ligand-binding domain, a transmembrane (TM) domain, and an intracellular kinase domain (Shiu and Bleecker 2001). The extracellular domain of RLK binds specific ligands of pathogens, and the intracellular kinase domain transduces signals to downstream components by phosphorylation, activating the defense response (Morillo and Tax 2006; Osakabe et al. 2013). RLKs can be divided into more than 44 subfamilies, depending on the variation of the extracellular domain (Dardick et al. 2012; Gish and Clark 2011). The leucine-rich repeat (LRR)-RLK, the largest subclass of RLKs, with 235 members in *Arabidopsis* and 309 members in rice, plays important roles in mediating plant responses to organ growth, environmental cues, and hormone and stress perception (Afzal et al. 2008; Kim and Wang 2010; Kinoshita et al. 2010; Shpak et al. 2005). In addition, some LRR-RLKs may also be involved in regulating plant responses to biotic stresses, including *FLS2*, *EFR*, and *Xa21* (Antolín-Llovera et al. 2012; Bauer et al. 2001; Shiu and Bleecker 2001). *FLS2*, a well-studied plant pattern-recognition receptor (PRR), perceives and binds bacterial flagellin (flg22), resulting in the signal transduction to intracellular and amplification by the mitogen-activated protein kinase cascade response with the phosphorylation of intracellular kinases, and *WRKY22* and *WRKY29* act in the downstream of *FLS2* to activate defense-related genes (Tang et al. 2017). *EFR*, a cell-surface receptor-like kinase of *Arabidopsis thaliana*, recognizes an epitope (elf18) of bacteria, activating plant defense responses (Schoonbeek et al. 2015; Zipfel et al. 2006). *Xa21*, encoding a TM receptor kinase, is the first bacterial blight resistance gene cloned from rice and has received much attention because of its broad-spectrum resistance against *Xanthomonas oryzae* pv. *oryzae* (Peng et al. 2008; Pruitt et al. 2015). Recent studies showed that OsWRKY62 could interact with the intracellular domain of Xa21 in the rice protoplast nucleus. Therefore, a new possible immune receptor model was proposed, i.e., a kinase is transferred into the nucleus and interacts with a transcriptional regulator directly after the receptor has recognized conserved microbial signatures (Peng et al. 2008).

In the present study, we identified and cloned a homolog of the rice *Xa21* in wheat, named *TaXa21*, which was significantly up-regulated in the HTSP resistance of XY 6 to *P. striiformis* f. sp. *tritici* and shared 59% similarity in amino acids with the rice *Xa21*. The transcript profile of *TaXa21* was analyzed under different hormone treatments and its subcellular localization was determined. Additionally, interactions between partial domains of *TaXa21* and *TaWRKY62* and, also, of *TaWRKY76* and *TaWRKY62* were studied. To confirm whether *TaXa21* participates in HTSP resistance to *P. striiformis* f. sp. *tritici*, knockdown of *TaXa21* by virus induced gene silencing (VIGS) was performed to study subsequent host resistance against *P. striiformis* f. sp. *tritici*. Our results suggest that *TaXa21* is associated with *TaWRKY76* and *TaWRKY62* and involved in HTSP resistance to *P. striiformis* f. sp. *tritici*.

RESULTS

Cloning and sequence characterization of *TaXa21*.

Based on the transcriptome sequencing data, a 3,464-bp cDNA fragment was isolated from XY 6, using rapid amplification of cDNA ends (RACE). This gene encodes a 1,051–amino acid protein with an estimated molecular mass of 113.39 kDa and an isoelectric point (PI value) of 7.7. The protein is predicted to possess a signal-peptide domain, nine LRR domains, a TM domain, and a serine/threonine protein kinase catalytic domain, consistent with structural features of RLKs (Supplementary Fig. S1). Nucleic acid sequence analysis indicated that this protein shares 56% similarity in amino acids

with the rice *Xa21*. Therefore, we designated this gene as *TaXa21* (GenBank accession number MH891497). *TaXa21* shares 99.97% similarity in nucleotides with *TaXa21*-4BL in the IWGSC wheat genome database (Supplementary Fig. S2).

Expression of *TaXa21* in different tissues and in response to hormones and hydrogen peroxide.

TaXa21 expression in roots, stems, and leaves of XY 6 under normal conditions was quantified by quantitative reverse transcription (qRT)-PCR. The expression of *TaXa21* varied greatly with tissues in XY 6. The expression level in leaves was 5.3-fold and 12.5-fold of that in roots and stems, respectively (Fig. 1A).

To study the *TaXa21* expression patterns in response to different plant hormones, wheat leaves were treated with four hormones: salicylic acid (SA), abscisic acid (ABA), methyl jasmonate (MeJA), and ethanol (ET). Relative to expression at 0 h of each treament, the transcript of *TaXa21* increased by 5.2-fold after ET treatment for 0.5 h. Both ABA (for 2 h) and JA (for 0.5 h) treatments reduced the expression of *TaXa21*, but the SA treatment did not affect *TaXa21* expression (Fig. 1B). In addition, the *TaXa21* expression level was significantly induced by hydrogen peroxide (H_2O_2) at 2 h, with an approximate 6.5-fold increase.

Expression of *TaXa21* in HTSP resistance to *P. striiformis* f. sp. *tritici*.

To analyze *TaXa21* transcript profiles in HTSP resistance to *P. striiformis* f. sp. *tritici*, *TaXa21* expression was measured in leaf samples collected at 0 to 312 h postinoculation (hpi) with *P. striiformis* f. sp. *tritici*. As shown in Figure 2, the transcript levels of *TaXa21* in inoculated leaves were higher than in noninoculated leaves in the early stage of *P. striiformis* f. sp. *tritici* infection. After exposure to HT (20°C) at 192 hpi for 24 h, the expression of *TaXa21* in the HT samples was significantly higher at 204 and 216 hpi than in the normal temperature (NT, 15°C) samples; the level at 204 hpi was approximately 12-fold higher than the base level. The transcript level of *TaXa21* did not significantly differ between the HT and NT mock (noninoculated) treatments.

Suppression of *TaXa21* reduces HTSP resistance to *P. striiformis* f. sp. *tritici*.

Because *TaXa21* was related to the HTSP resistance to *P. striiformis* f. sp. *tritici*, we studied the effects of knocking down *TaXa21* on host response and *P. striiformis* f. sp. *tritici* development. Knocking down was achieved through barley stripe mosaic virus (BSMV)-based VIGS. The 3′ terminal 151-bp specific segment of *TaXa21* was inserted to BSMV:γ vector, designed as BSMV:*TaXa21*-as. Stripe mosaic symptoms were observed nine to 10 days after BSMV inoculation (Fig. 3A); the expression level of *TaXa21* was suppressed by 59 to 72% (Fig. 3d). Next, the fourth leaves of BSMV-inoculated seedlings were inoculated with *P. striiformis* f. sp. *tritici* race CYR32, and stripe rust symptoms and signs were assessed at 15 days postinoculation (dpi) with *P. striiformis* f. sp. *tritici*. XY 6 showed a susceptible response under the continuous NT (Fig. 3B), whereas, in seedlings exposed to HT for 24 h, uredia on the *TaXa21*-silenced leaves were more than those of nonsilenced leaves, which were then inoculated with BSMV:00 under HT as a control (Fig. 3C). Consistent with the phenotype, qRT-PCR analysis showed that the transcript level of *TaXa21* was upregulated after the HT treatment for 12 h in those nonsilenced leaves. Although *TaXa21* can be induced again by the HT treatment in the silenced leaves, the expression level was lower than that in the HT-treated nonsilenced plants at 24, 72, and 120 h post–temperature treatment (hptt) (Fig. 3E).

To determine whether the expression level of *P. striiformis* f. sp. *tritici* resistance-related genes in *TaXa21* knockdown leaves was affected, *TaACO* (ET pathway) and *TaCAT* (H_2O_2 pathway) were quantified with qRT-PCR. The *TaACO* transcript level was significantly higher in the HT-treated nonsilenced leaves than in the HT-treated *TaXa21*-silenced leaves at both 12 and 24 hpi (Fig. 3F). In contrast, the *TaCAT* transcript level was higher in the *TaXa21*-silenced leaves than in nonsilenced leaves at 48, 72, and 120 hpi; the highest level was in the NT-treated *TaXa21*-silenced plants (Fig. 3G).

Observation of *P. striiformis* f. sp. *tritici* growth and host response.

TaXa21-silenced XY 6 leaves were assessed microscopically at 48 and 120 hpi to determine hyphal length and number of haustorial mother cells (Fig. 4A to D). There were no obvious differences in the hyphal length and the number of haustorial mother cells at 48 and 120 hpi between the *TaXa21* knockdown plants and BSMV:00 control plants (Fig. 4E and F).

Pathogen development and host response were assessed microscopically in wheat leaves with different temperature treatments (Fig. 5A and B). Colony length in the HT-treated *TaXa21*-silenced leaves significantly decreased compared with the NT-treated *TaXa21*-silenced at 24 hptt (Fig. 5D). A large number of uredinia were observed at 120 hptt; the uredinium length was significantly shorter in the HT-treated *TaXa21*-knockdown leaves than in the NT-treated *TaXa21*-knockdown leaves (Fig. 5C). In addition, there were fewer necrotic cells in the *TaXa21*-knockdown leaves than in the control leaves at 48 and 120 hptt (Fig. 5E).

Subcellular location of TaXa21-GFP fusion protein.

The predicted TaXa21 protein sequence contains an extracellular receptor domain, a single TM domain, and a C-terminal cytoplasmic serine/threonine protein kinase domain, indicating that TaXa21 could be a plasma membrane protein. To confirm this inference, the fusion construct pCambia1302:TaXa21-GFP and the control vector pCambia1302:GFP were transformed into tobacco (*Nicotiana benthamiana*) cells. When TaXa21-GFP fusion protein was expressed in the tobacco cells through agrobacterium-mediated transformation, adding proteasome inhibitor MG132 led to accumulation of TaXa21 protein (Fig. 6A), indicating that TaXa21 protein was degraded by the ubiquitin-proteinase pathway. Green fluorescent protein (GFP) was diffusely distributed throughout the host cells, while green fluorescence produced by the TaXa21-GFP and red fluorescence produced by the AtPIP2A-mcherry protein overlapped in the plasma membrane with MG132, showing that TaXa21 is located in plasma membrane (Fig. 6B).

Interactions among TaXa21, TaWRKY76, and TaWRKY62.

To determine whether interactions between TaXa21 and TaWRKY76 and between TaXa21 and TaWRKY62 occur and are involved in the host defense response, yeast two-hybrid was performed. We noticed that BD-TaWRKY76 exhibited a weak autoactivation activity, which was abolished by adding 10 mM 3-amino-1, 2, 4-triazole (3AT). A truncated TaXa21, carrying a TM domain and a kinase domain, was fused with bait vector pGBKT7, and TaWRKY76 and TaWRKY62 were fused with prey vector pGADT7. Interaction was observed between
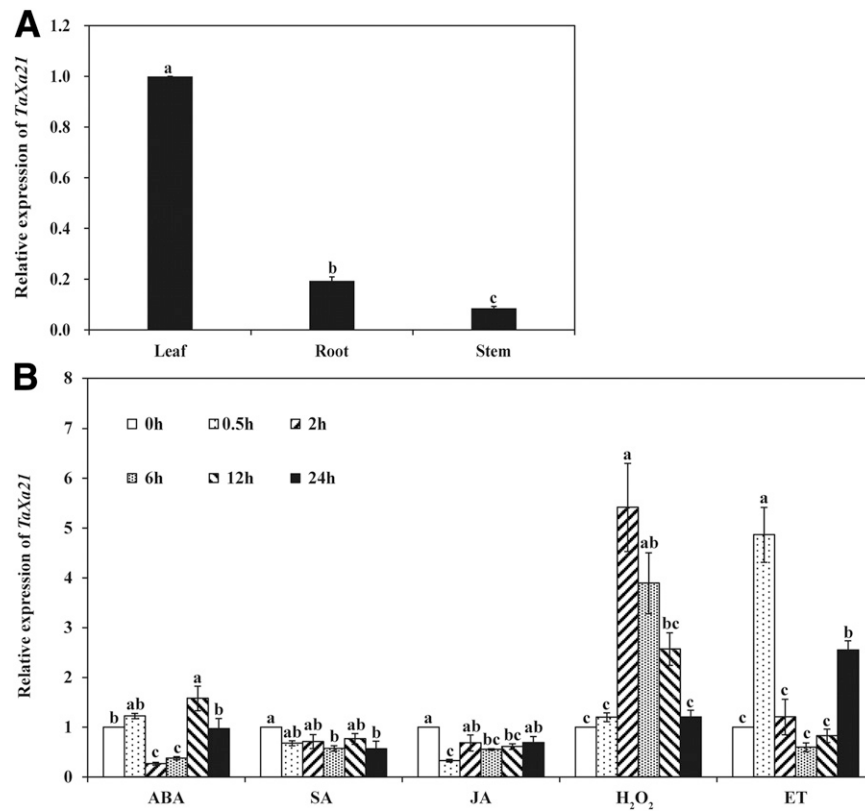
Fig. 1. Expression pattern of *TaXa21* in wheat cultivar Xiaoyan 6 leaves as quantified by quantitative reverse transcription (qRT)-PCR. **A,** Transcript level of *TaXa21* in the leaf, stem, and root issues. **B,** Transcript profiles of *TaXa21* after hormone and H_2O_2 treatments. The transcriptional level was determined by qRT-PCR with *Ta26s* as a reference gene. Hormone elicitors: ABA, abscisic acid; SA, salicylic acid; MeJA, methyl jasmonate; ET, ethylene. H_2O_2, hydrogen peroxide. The mock control was treated with 0.1% (vol/vol) ethanol solution. The expression level of *TaXa21* at 0 h was normalized as 1 for each treatment. Analysis of variance was followed by the Duncan's multiple comparison test. The error bar represents the standard errors (three replicates). Duncan's multiple comparison test was conducted at the different timepoints within each treatment; *TaXa21* expression levels do not differ significantly if they contain at least one common lowercase letter between timepoints for each treatment.

BD-TaXa21-F1 and AD-TaWRKY76, indicated by the yeast growth on the synthetic dropout (SD) medium lacking Leu, Trp, and His supplemented with 10 mM 3AT. No interactions were detected between TaXa21-F1 and TaWRKY62 (data not shown). To determine whether the TM domain of TaXa21 is essential for its interaction with TaWRKY76, only the kinase domain of TaXa21 was fused with pGBKT7 and transformed together with the AD-TaWRKY76 into AH109 yeast competent cells. No yeast growth was observed, suggesting that the interaction between TaXa21 and TaWRKY76 requires the TM domain. In addition, we also confirmed that TaWRKY76 could interact with TaWRKY62 in the yeast (Fig. 7B).

To validate whether TaXa21 interacts with TaWRKY76 in planta, different regions of TaXa21, were fused with the C-terminal fragment of the yellow fluorescent protein (YFP^C); and TaWRKY76 and TaWRKY62 were fused with a N-terminal fragment of the yellow fluorescent protein (YFP^N). Fluorescence was predominantly detected in nuclei and cell membranes when TaXa21-F1-YFP^C and TaWRKY76-YFP^N were expressed transiently in tobacco (Fig. 7C). These results indicated that the TM and kinase domains of TaXa21 could interact with full-length TaWRKY76 in nuclei and cell membranes. Meanwhile, the interaction between full-length TaWRKY76 and TaWRKY62 in nuclei was observed.

To determine whether TaWRKY76 and TaWRKY62 are localized in nuclei or enter nuclei from cytoplasma after interactions with other proteins, we conducted subcellular localization experiments in tobacco cells. Green fluorescence produced by the TaWRKY76-GFP and TaWRKY62-GFP (Fig. 7D) fusion protein and red fluorescence produced by the AtH$_2$B-mcherry protein overlapped in nuclei, indicating a nuclear localization of TaWRKY76 and TaWRKY62.

DISCUSSION

Plants can be infected by various pathogens and specific host defense mechanisms have been evolved to cope with these pathogens. Plants recognize PAMPs by PRRs, resulting in PTI responses (Rodriguez et al. 2010). To suppress PTI, pathogens produce specific pathogen proteins called effectors. Plants can also recognize effectors by specific resistance (R) genes,

leading to ETI responses (Chisholm et al. 2006). Accumulating evidences indicate that LRR-RLKs play important roles in the signaling pathway in the host-pathogen interactions.

In the present study, we determined that *TaXa21* is a LRR-RLK and involved in HTSP resistance to *P. striiformis* f. sp. *tritici* in wheat. The transcription level of *TaXa21* increased after the HT treatment and downregulation of *TaXa21* expression compromised the HTSP resistance to *P. striiformis* f. sp. *tritici*, indicating that *TaXa21* functions as a positive regulator of the HTSP resistance to *P. striiformis* f. sp. *tritici*. The *TaXa21* expression in the HT-treated leaves was higher than in the HT mock and NT treatments 12 hptt, which was earlier than *TaWRKY70* (24 hptt). Therefore, we speculate that *TaXa21* is located upstream of the signaling pathway and is responsible for perceiving environmental signals and transmitting them downstream such as to WRKY transcription factors. Further research is needed to determine whether *TaXa21* in HTSP resistance to *P. striiformis* f. sp. *tritici* causes PTI or ETI responses.

Numerous studies have demonstrated that transcriptional levels of many LRR-RLKs change upon various exogenous hormone treatments (Chae et al. 2009; ten Hove et al. 2011). In the current study, *TaXa21* was down-regulated in response to ABA and JA but induced by ET. Moreover, a key enzyme, *TaACO*, in the ET biosynthesis pathway was significantly reduced in TaXa21-knockdown HT-treated plants at 12 and 24 hptt, indicating that *TaXa21* is involved in the ET-mediated HTSP resistance to *P. striiformis* f. sp. *tritici*. These results suggest that *TaXa21* functions at the nexus of biotic and abiotic stress signals.

Signal transduction through the interaction between WRKY transcription factors and pathogen sensors is important in host-pathogen interactions. For example, MLA10 in barley, belonging to the coiled coil-nucleo binding-LRR-type of R proteins, induces ETI against *Blumeria graminis* f. sp. *hordei* by interacting with HvWRKY1 and HvWRKY2 in nuclei. Upon *B. graminis* f. sp. *hordei* infection, HvWRKY1 and HvWRKY2 can change from transcriptional repressors to transcriptional activators by binding MLA10, resulting in plant defense responses (Shen et al. 2007). In rice, *pb1*, a panicle blast resistance gene, was reported to interact with *OsWRKY45*
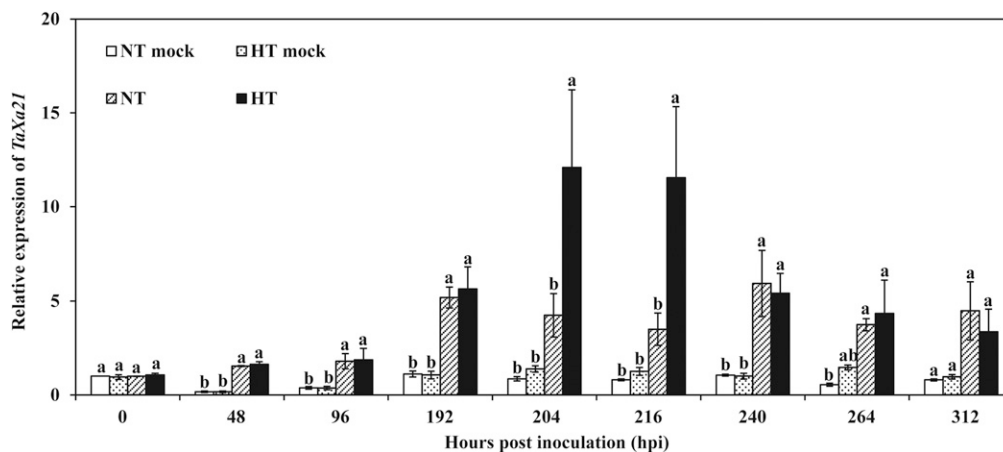
Fig. 2. Quantitative reverse transcription (qRT)-PCR analysis of *TaXa21* in response to *Puccinia striiformis* f. sp. *tritici* and temperature. NT mock = normal temperature noninoculated leaves under constant temperature (15°C); HT mock = high-temperature noninoculated leaves with 24-h exposure to high temperature of 20°C 192 h postinoculation (hpi) with *P. striiformis* f. sp. *tritici* (the initial stage of *P. striiformis* f. sp. *tritici* development); NT = leaves inoculated with *P. striiformis* f. sp. *tritici* under 15°C; HT = leaves inoculated with *P. striiformis* f. sp. *tritici* but with 24-h exposure to 20°C 192 hpi. The transcriptional level was determined by qRT-PCR with *Ta26s* as a reference gene and was relative to the level at 0 hpi of NT mock for all treatments. The error bar represents the standard errors (three replicates). Duncan's test was conducted among treatments at the same timepoint. There were no significant differences between treatments at the same timepoint sharing at least one lowercase letter.

in nuclei; and *pb1*-mediated panicle blast resistance was largely compromised when *WRKY45* was knocked down. In addition, wheat wXa21-like1 and wXa21-like2, in which amino acids share 82 and 78% similarities with TaXa21, can interact with WRKY76 slightly in yeast cells (Cantu et al. 2013). In the present study, we demonstrated that the intact TM and kinase domains of TaXa21 can interact with TaWRKY76 in nuclei and membrane. In addition, TaWRKY76-TaWRKY62 interactions were also observed in nuclei. Previously, we showed that *TaWRKY62* positively regulates HTSP resistance to *P. striiformis* f. sp. *tritici* (Wang et al. 2017b) and that TaWRKY70 plays a positive role in HTSP resistance (Wang et al. 2017a). We also failed to detect any interaction between TaWRKY70 and TaXa21 (data not shown). Based on these results, we
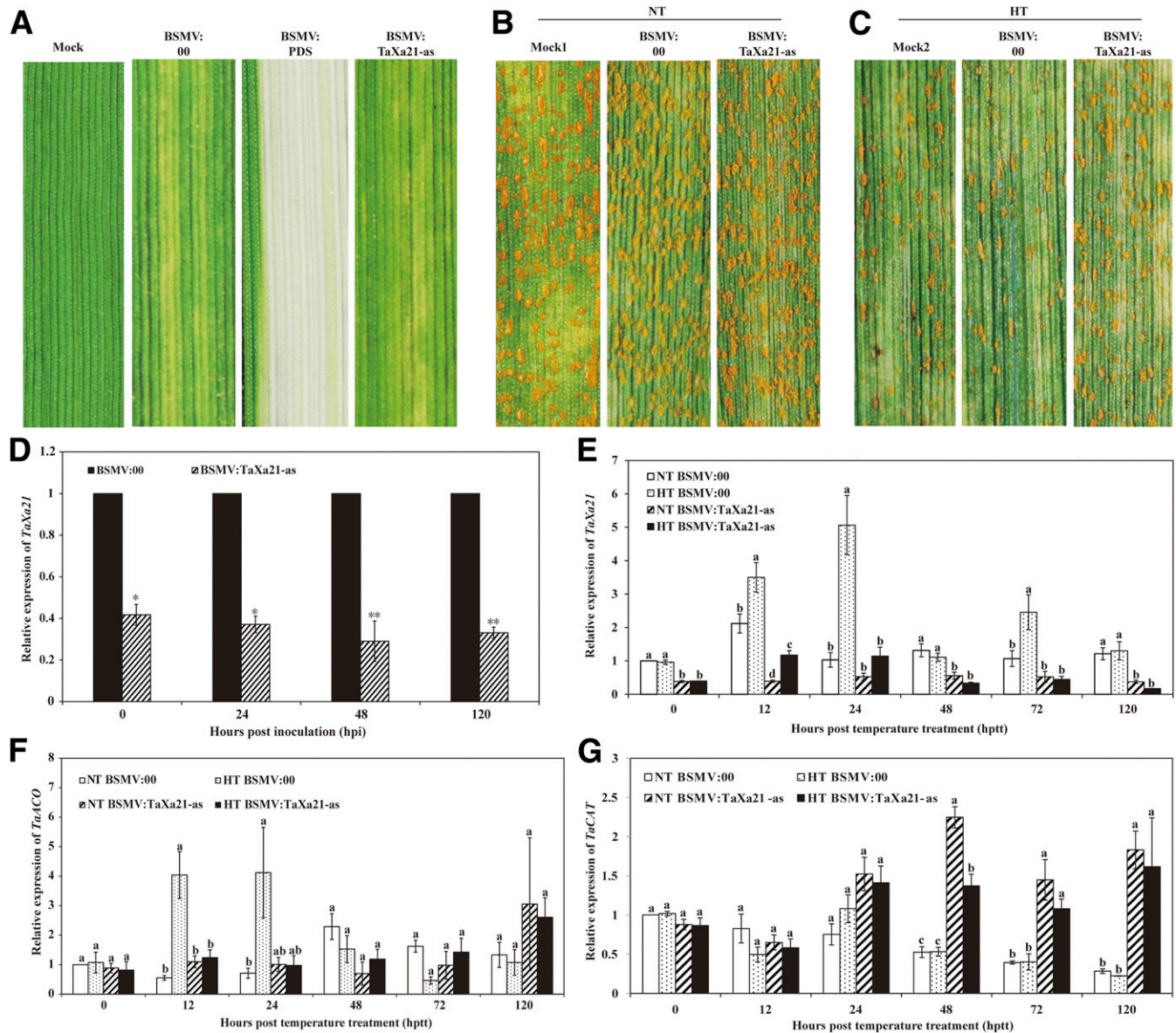
Fig. 3. *TaXa21* plays a positive role in the high-temperature seedling plant resistance to *Puccinia striiformis* f. sp. *tritici* in wheat cultivar Xiaoyan 6 (XY 6) as indicated by barley stripe mosaic virus (BSMV)-induced silencing. **A,** Mild chlorotic mosaic and photo-bleaching symptoms on fourth leaves of XY 6 at 9 to 11 days postinoculation with BSMV:00 and BSMV:PDS (phytoene desaturase), respectively. Mock = leaves of XY 6 inoculated with the 1× FES buffer (0.1 M glycine, 0.06 M K_2HPO_4, 1% (wt/vol) tetrasodium pyrophosphate, 1% (wt/vol) bentonite, and 1% (wt/vol) celite, pH 8.5). **B** and **C,** The *TaXa21*-silenced and nonsilenced leaves were all inoculated with *P. striiformis* f. sp. *tritici* race CYR32, were transferred to normal temperature (NT) (B) and high temperature (HT) (C) treatments during the 192 h postinoculation (hpi) (the initial *P. striiformis* f. sp. *tritici* symptom expression stage), and were assessed at 336 hpi. **D,** Relative transcript level of *TaXa21* in the *TaXa21*-silenced leaves inoculated with CYR32 under NT. Leaves of XY 6 infected with BSMV:00 or BSMV:*TaXa21*-as were collected at 0, 24, 48, and 120 hpi with CYR32 (*t* test, two asterisks (**) indicate *P* < 0.01). The data were standardized with the *Ta26s* gene. The transcript level of *TaXa21* in the leaves with BSMV:00 at each timepoint was standardized as 1. **E,** Transcript abundances of *TaXa21* in response to temperature and *P. striiformis* f. sp. *tritici* inoculation in the *TaXa21*-silenced and nonsilenced leaves. RNA samples were isolated from wheat leaves preinoculated with BSMV at 0, 12, 24, 48, 72, and 120 h post–temperature treatment (hptt) after inoculation with CYR32; 0 hptt was the starting time of the HT treatment. **F,** Transcript analysis of defense-related genes *TaACO* and **G,** *TaCAT* after *P. striiformis* f. sp. *tritici* inoculation and temperature treatments in the *TaXa21*-silenced and nonsilenced leaves. *TaCAT* = catalase, *TaACO* = 1-aminocyclopropane-1-carboxylate oxidase. The transcriptional level was determined by quantitative reverse transcription-PCR with *Ta26s* as a reference gene. Treatment comparison was based on the Duncan's multiple range test; standard errors were based on three replicates. The expression levels of *TaXa21* (E), *TaACO* (F), and *TaCAT* (G) in NT-treated nonsilenced leaves at 0 hptt were standardized as 1. Duncan's test was conducted among treatments at the same timepoint. There were no significant differences between treatments at the same timepoint if they shared at least one common lowercase letter.

propose two possible models for the interaction regions of TaXa21 and TaWRKY76. In the first model, upon *P. striiformis* f. sp. *tritici* infection and HT treatment, the TM and activated kinase domains of TaXa21 are cleaved from the membrane, move into nuclei, and interact with TaWRKY76; the signal is then further transmitted through the TaWRKY76-TaWRKY62 interaction. In the second model, *P. striiformis* f. sp. *tritici* inoculation and HT treatment lead to activation of the TaXa21 kinase domain, which phosphorylates TaWRKY76 through their interaction in the cell membrane; the phosphorylated TaWRKY76 proteins are translocated into the nuclei, combine with TaWRKY62, and regulate downstream cascading gene expressions. The evidence to support the second model comes from the Jak-STAT pathway (Darnell et al. 1994). The TM receptor could recognize interferon (IFN), leading to activation of the JAK kinase of receptors and, then, phosphorylation of the STAT protein through the Jak-STAT interaction in the cell membrane. The phosphorylated STAT proteins are translocated to the nuclei, combining with downstream targets and regulate immune responses.

WRKY transcription factors (TFs) contain a DNA-binding domain and can bind to the W-box repeats of promoters in defense-related genes; the interactions between different WRKY TFs alter the activity of sequence-specific DNA binding, leading to varying degrees of plant defense responses. The interaction of WRKY18 with WRKY40 or WRKY60 may have enhanced their DNA-binding activity, which may contribute to their roles in disease resistance (Xu et al. 2006). We previously showed that *TaWRKY62* plays a positive role in the HTSP resistance to *P. striiformis* f. sp. *tritici* in XY 6 (Wang et al.

2017b); the present study confirmed its interaction with *TaWRKY76*. Further research is needed to determine whether the interaction between *TaWRKY76* and *TaWRKY62* can change the ability of DNA binding and enhance the defense response.

In summary, we showed differences between homologous gene *Xa21* in rice and *TaXa21* in wheat. Unlike the rice Xa21, whose kinase domain could interact with OsWRKY62 in nuclei, the TM and kinase domains of TaXa21 can interact with TaWRKY76 instead of TaWRKY62 in the membrane and nuclei and the intact TM domain is essential for their interaction. Whether these differences are consistent with our two proposed models needs further investigations. TaWRKY62, a positive regulator in HTSP resistance to *P. striiformis* f. sp. *tritici*, interacts with TaWRKY76 in nuclei. Thus, we speculate that, upon *P. striiformis* f. sp. *tritici* infection and HT treatment, the extracellular signal is received by the LRR domain of TaXa21 with kinase domain phosphorylation and transmits to TaWRKY62 through TaWRKY76, leading to the ET-mediated defense responses.

MATERIALS AND METHODS

Plant materials, inoculations, and treatments.

Wheat (*Triticum aestivum*) cultivar XY 6 and *P. striiformis* f. sp. *tritici* race CYR32 were used throughout this study. Plants were grown, inoculated and exposed to different temperatures based on previously published protocols (Wang et al. 2017a).

For hormone and hydrogen peroxide treatments, 14-day-old wheat seedlings were sprayed with 100 µM SA, 100 µM MeJA, 100 µM ET, 100 µM H_2O_2, and 100 µM ABA (Zhang et al.
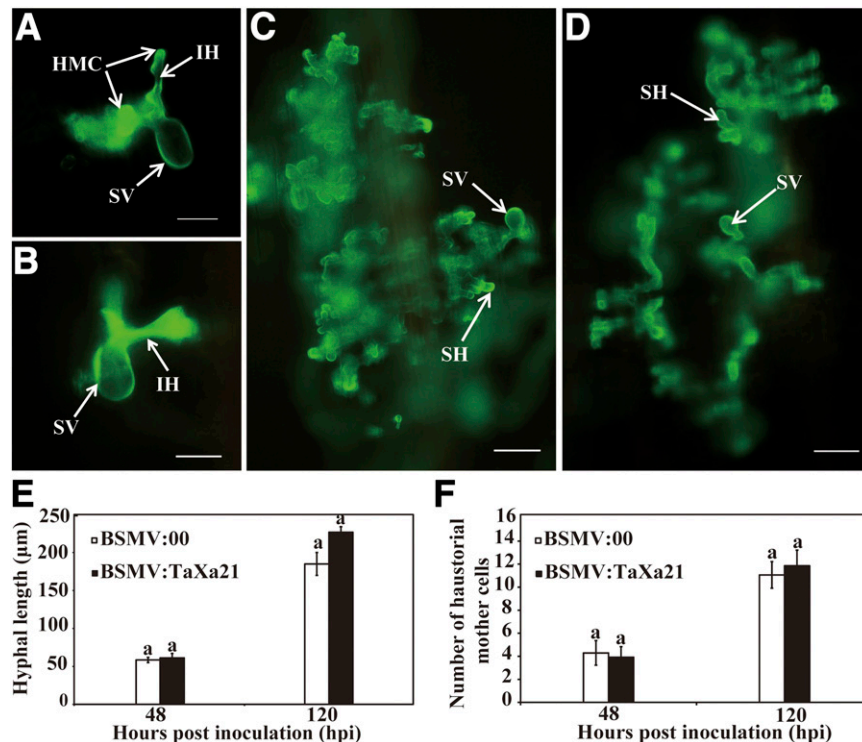
Fig. 4. Histological observation of fungal growth and host response in wheat leaves treated with barley stripe mosaic virus (BSMV) and inoculated with race CYR32 of *Puccinia striiformis* f. sp. *tritici* strain under normal temperature (NT). **A through D,** The fourth wheat leaves were challenged with *P. striiformis* f. sp. *tritici* in BSMV:00- (A and C) and BSMV: *TaXa21*-as (B and D)-inoculated leaves. Photographs were taken under an epifluorescent microscope at 48 h postinoculation (hpi) with *P. striiformis* f. sp. *tritici*. Bars = 20 µm (A and B) and, at 120 hpi, 50 µm (C and D). SV = substomatal vesicle, IH = initial hyphae, HMC = haustorial mother cell. **E,** Hyphal length and **F,** number of haustorial mother cells in wheat leaves treated with BSMV and inoculated with race CYR32 of *P. striiformis* f. sp. *tritici* at 48 and 120 hpi under NT. Hyphal length in the average distance from the junction of the substomatal vesicle and the hyphal tip. Mean values and standard error were calculated from three replicates. Duncan's test was conducted among treatments at the same timepoint. There were no significant differences between each treatment at the same timepoint if they shared at least one common lowercase letter, on the basis of the Duncan's multiple range test.

2004) and were sampled at 0, 0.5, 2, 6, 12, and 24 hpi (0 hpi: just before treatment). All chemicals were dissolved in 0.1% (vol/vol) ethanol. The mock seedlings were treated with 0.1% (vol/vol) ethanol solution. The mean expression values of *TaXa21* at 0 hpi for each treatment were converted to 1 to normalize the expression values of the same genes at the other timepoints for comparison. For tissue-specific expression analysis of *TaXa21*, roots, stems, and leaves were sampled at the two-leaf stage. All samples were frozen in liquid nitrogen and stored at –80°C for RNA extraction. For every sampling point, there were three biological replicates.

To evaluate the expression levels of *TaXa21* in HTSP resistance to *P. striiformis* f. sp. *tritici*, wheat leaves were harvested at 0, 48, 96, 192, 194, 198, 204, 216, 240, 264, and 312 hpi (HT was applied at 192 hpi for 24 h). Plants allocated to the mock-inoculation control were inoculated with sterile water. There were three biological replicates for each treatment at each sampling timepoint.

Identification and sequence analysis of *TaXa21*.

Based on transcriptome sequences, RACE primers (Supplementary Table S1) were designed to clone the 5′ and 3′ terminal sequences of *TaXa21*. Amplification of cDNA ends was performed using the SMART RACE cDNA amplification kit

(Clontech). Specific primers were designed to obtain the full length of *TaXa21*, *TaXa21*-F, and *TaXa21*-R. The PCR product was cloned into the PMD18-T vector (TaKaRa, Tokyo) for sequencing. Protein molecular weight and PI were predicted with the DNAMAN6.0 software.

RNA isolation and qRT-PCR.

Total RNA from leaves of each sample was extracted using the SV total RNA isolation system (Promega) following manufacturer instructions. Total RNA (1,000 ng) was subjected to first-stand cDNA synthesis with the PrimeScript RT reaction system (TaKaRa). qRT-PCR was performed to quantify *TaXa21* expression, using UltraSYBR mixture (Kangwei, Beijing) in a volume of 25 µl; the *Ta26s* gene (ATP-dependent *26s* proteasome regulatory subunit) (Unigene number Ta22845) was used as an internal reference. Relative transcript levels of *TaXa21* were calculated by the comparative cycle threshold ($2^{-\Delta\Delta Ct}$) method. The expression level was assessed from three replicates.

BSMV-mediated Ta*Xa21* silencing.

A specific 151-bp cDNA was amplified with primers containing the *Not*I and *Pac*I restriction enzyme sites and was inserted into the BSMV:r vector to form recombinant plasmid BSMV:*TaXa21*-as. Transcription in vitro was conducted using
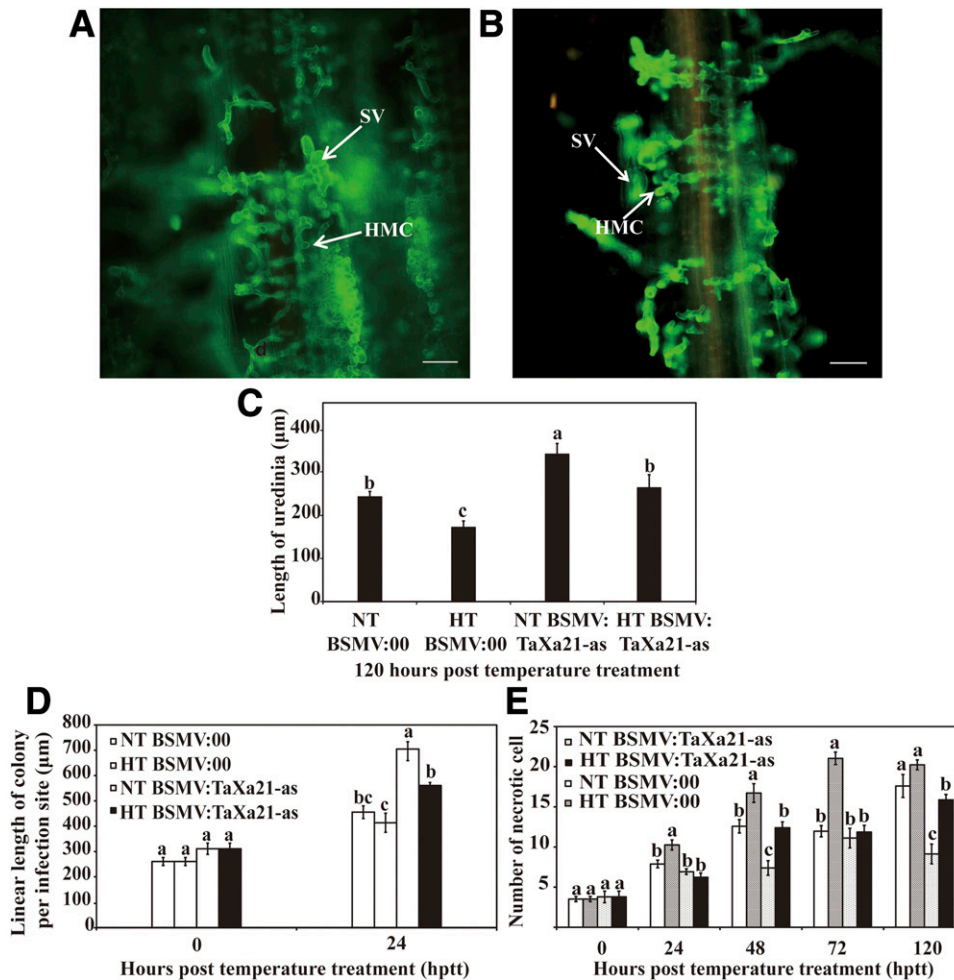
Fig. 5. Histological observation of race CYR32 of *Puccinia striiformis* f. sp. *tritici* development and wheat response in the *TaXa21*-silenced and control leaves leaves under **A,** normal temperature (NT) and **B,** high temperature (HT) during the initial symptom expression stage of *P. striiformis* f. sp. *tritici* development. Photographs were taken under an epifluorescent microscope. SV = substomatal vesicle, HMC = haustorial mother cell. Bars = 50 µm. **C,** Uredinium length, **D,** linear length of colony per infection sites and **E,** numbers of necrotic cells were all recorded from 30 to 50 infection sites. Mean values and standard error were calculated from three replicates. Duncan's test was conducted among treatments at the same timepoint. There were no significant differences between treatments at the same timepoint if they share at least one common lowercase letter, on the basis of the Duncan's multiple range test.

linearized products of α, β, γ, γ-PDS (phytoene desaturase) or γ-*TaXa21* as a template. BSMV virus vectors (α, β, and γ) or BSMV recombinant virus vectors (α, β, γ-PDS, and α, β, and γ-*TaXa21*) were inoculated onto the second leaves of wheat seedlings. Seedlings inoculated with BSMV:γ and BSMV:PDS were used as negative and positive controls, respectively. The control plants were inoculated with 1× FES buffer (0.1 M glycine, 0.06 M K_2HPO_4, 1% (wt/vol) tetrasodium pyrophosphate, 1% [wt/vol] bentonite, and 1% [wt/vol] celite, pH 8.5). After inoculation, seedlings were kept at 25°C in the dark for 24 h and were subsequently maintained in a growth chamber at 25 ± 1°C with a 16-h photoperiod. The fourth leaves with BSMV-inoculated were inoculated with *P. striiformis* f. sp. *tritici* CYR32, and seedlings were then maintained at 16 ± 1°C. *P. striiformis* f. sp. *tritici* development was assessed 14 dpi. For estimation of silencing efficiency of *TaXa21*, leaves inoculated with CYR32 were collected at 0, 24, 48, and 120 hpi and the expression level of *TaXa21* was quantified.

### Determine the effect of HT on expression of *TaXa21*.

To determine the effect of HT on *TaXa21* expression in *TaXa21*-silenced seedlings, two temperature treatments were applied to seedlings (including both *TaXa21* nonsilenced and silenced seedlings): i) for the HT treatment, seedlings were exposed to 20°C at 8 dpi for 24 h (the late incubation stage of *P. striiformis* f. sp. *tritici*) and were then maintained at 15°C; ii) for the continuous NT treatment, seedlings were maintained at 15°C all the time. Leaves from seedlings subjected to HT or NT treatments were sampled at 0, 12, 24, 48, 72, and 120 hptt to determine the transcript level of *TaXa21* (0 hptt is the starting point of HT treatment). In addition, expression levels of two selected genes (*TaCAT* and *TaACO*) in the H_2O_2 and ET signaling pathways were quantified at 0, 12, 24, 48, 72, and 120 hptt.

Histological observation of *P. striiformis* f. sp. *tritici* development and wheat response.

Wheat leaves were sampled at 48 and 120 hpi to measure hyphal length and estimate the number of haustorial mother cells. BSMV-treated leaves were sampled 0, 24, 48, 72, and 120 hptt for assessment of colony length, uredinium length, and the number of necrotic cells. Staining was performed following the method of Cheng et al. (2015). Hyphal length and the number of haustorial mother cells were determined under ultraviolet excitation with a fluorescent microscope. Cell death was assumed if autofluorescence was observed at the infection sites. For each treatment at each sampling timepoint, 30 to 50 infection sites from randomly chosen 8- to 10-leaf segments were randomly selected for assessment. The hyphal length, colony length, and uredinium length were estimated using the DP-BSW software connecting to an Olympus BX51 microscope. Student's *t* test was used to compare treatment effects at each timepoint, using SAS software (SAS Institute Inc.).

Subcellular localization of TaXa21, TaWRKY76, and TaWRKY62.

The full coding region of *TaXa21*, *TaWRKY76*, and *TaWRKY62* without the stop codon was amplified with gene-specific primers and was cloned into the pCambia1302-GFP vector via *Nco*I and *Spe*I digestion, yielding pCambia-TaXa21-GFP, pCambia-TaWRKY76-GFP, and pCambia-TaWRKY62-GFP, respectively. Three recombination vectors and the control vector pCambia1302-GFP were transformed into *Agrobacterium tumefaciens* GV3101. Transformed *A. tumefaciens* cells containing recombination vector or pCambia1302-GFP were separately injected into the surface of tobacco leaves as previously described (Bracha-Drori et al. 2004). H_2B-mcherry fusion and the PIP2A-mcherry fusion proteins were used as
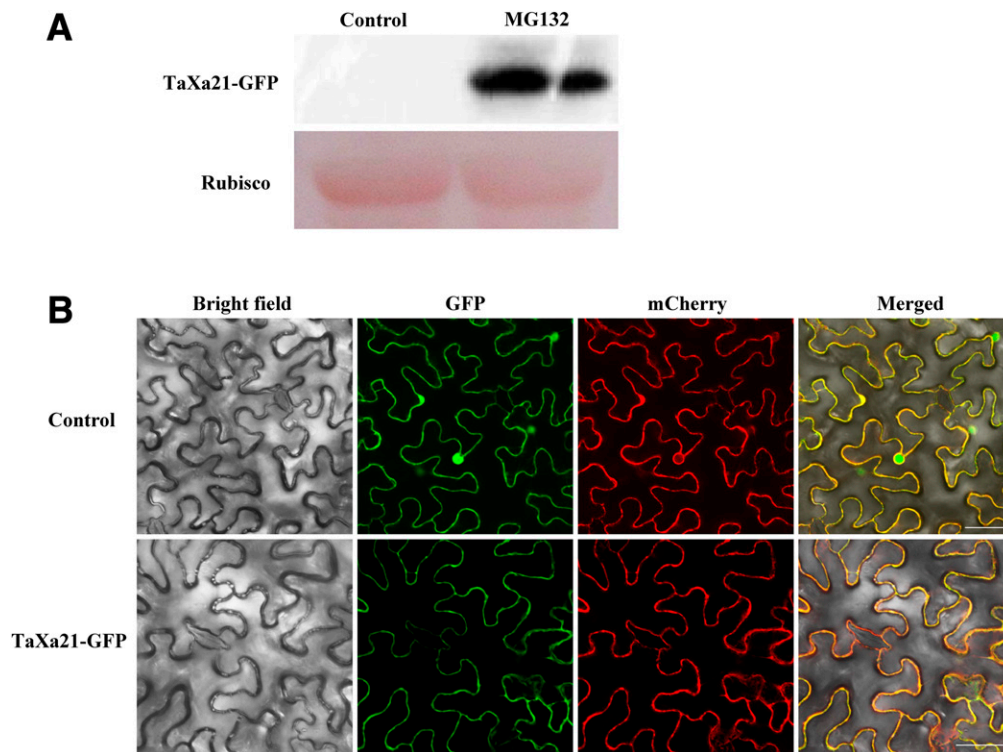
Fig. 6. Subcellular localization of TaXa21. **A,** TaXa21-GFP fusion protein expressed in tobacco (*Nicotiana benthamiana*) cells with (control) or without MG132 and detected by Western blot with Ponceau S staining. **B,** Images taken under a fluorescent microscope. Bright field represents the tobacco cells. Green fluorescent protein (GFP) (control) and TaXa21-GFP fusion protein were expressed in the tobacco cells, respectively. AtPIP2A protein, an aquaporin, was used as a plasma membrane location marker gene. Bar = 50 μm. Green fluorescence represents the location of GFP and TaXa21-GFP protein; red fluorescence represents the location of mcherry-AtPIP2A; bright field represents the tobacco cells; merge represents an overlap between green and red fluorescence. The large subunit of Rubisco was the loading control.

nuclear and plasma membrane markers, respectively. Tobacco leaves were fully infiltrated with injection of 50 μM MG132 at 12 h before sampling. The infiltrated tobacco leaves were observed under a fluorescent microscope within two to three days.

Protein extraction and Western blot.

Total protein was extracted from 500 mg of tobacco leaves transformed with *A. tumefaciens* containing the pCambia-TaXa21-GFP vector with or without MG132 injection with 1 ml of extraction buffer (50 mM Tris-HCl, pH 7.5, 150 mM NaCl, 5 mM EDTA, 3 mM dithiothreitol, 0.5% Triton X-100, 1 mM phenylmethylsulfonyl fluoride) and was separated by sodium dodecyl sulfate-polyacrylamide gel electrophoresis. GFP protein was detected with the anti-GFP antibody (Sigma). The large subunit of Rubisco was used as a loading control.
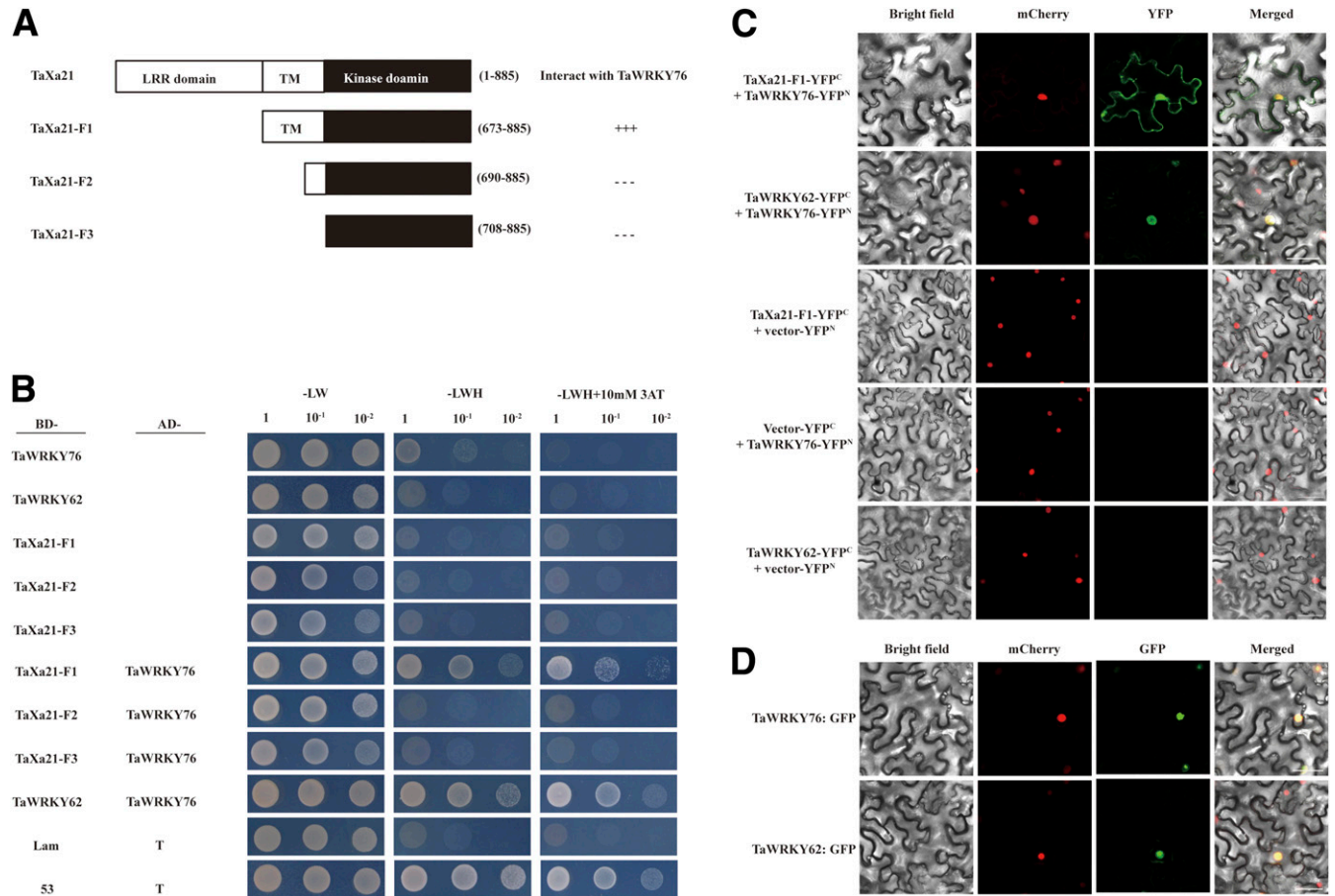
Yeast two-hybrid.

The bait and prey vectors were generated by inserting DNA fragments to pGBKT7 and pGADT7 plasmids, respectively. The transformed AH109 yeast cells harboring various combinations of bait and prey constructs were selected on SD medium lacking Leu and Trp and were then transferred to SD medium without Leu, Trp, and His to detect the selfactivation. Interaction was determined with yeast cells containing different plasmid combinations grown on SD medium without Leu, Trp, and His supplemented with 10 mmol 3-amino-1, 2, 4-triazole per liter, using a concentration selected based on the self-activation test.

Bimolecular fluorescence complementation assay.

The TaXa21-F1, TaXa21-F2, and TaXa21-F3 segments were cloned with specific primers and were fused with YFP^C to form TaXa21-F1-YFP^C, TaXa21-F2-YFP^C, and TaXa21-F3-YFP^C, respectively. The full-length coding sequences of TaWRKY76 and TaWRKY62 were cloned and fused with YFP^N to form TaWRKY76-YFP^N and TaWRKY62-YFP^N. The same method was used to construct TaWRKY62-YFP^C.

The constructed plasmids were transformed into *A. tumefaciens* GV3101 cells and were then coinfiltrated into the leaves of 4-week-old tobacco plants in different combinations. YFP fluorescence was observed using a laser scanning microscope

Fig. 7. Analysis of interaction among TaXa21, TaWRKY76, and TaWRKY62. **A,** Schematic diagrams of TaXa21-F1, TaXa21-F2, and TaXa21-F3, used in the analysis of interaction. **B,** Yeast two-hybrid assay. For autoactivation test, TaWRKY76, TaWRKY62, TaXa21-F1, TaXa21-F2, and TaXa21-F3 were fused with pGBKT7. For analysis of interaction, TaXa21-F1, TaXa21-F2, TaXa21-F3, and TaWRKY62 were fused with pGBKT7 to generate bait constructs; TaWRKY76 was fused with pGADT7 to generate prey construct. AH109 yeast cells with serial dilutions (1, 10^{-1}, and 10^{-2}) were incubated in synthetic dropout medium lacking Leu and Trp (–LW), Leu, Trp, His (–LWH), or Leu, Trp, His (–LWH) supplemented with 10 mmol of 3-amino-1, 2, 4-triazole per liter. Yeast cells containing pGADT7-T and pGBKT7-53 or pGBKT7-Lam vectors were used as positive and negative control. **C,** Fluorescence complementation assay analysis of TaXa21 and TaWRKY76 and TaWRKY62 and TaWRKY76 interactions. TaXa21 and TaWRKY62 were fused with C-terminal domain of the yellow fluorescence protein (YFP). TaWRKY76 was fused with N-terminal domain of the YFP. The two different combinations of plasmids were transformed into the cells of tobacco (*Nicotiana benthamiana*). The images were taken 72 to 96 h after infiltration. AtH$_2$B, a histone protein, was used as a nuclear location marker gene. The AtH$_2$B-mcherry protein also shows red fluorescence in the nucleus. Merge shows an overlap between yellow and red fluorescence. The leaf cells of tobacco containing TaXa21-F1-YFP^C+ YFP^N, YFP^C+TaWRKY76-YFP^N, and TaWRKY62-YFP^C+YFP^N were used as negative controls. **D,** Subcellular localizations of TaWRKY76 and TaWRKY62. Tobacco (*Nicotiana benthamiana*) cells transformed with TaWRKY76-GFP and TaWRKY62-GFP fusion protein, respectively. Images were taken under an epifluorescent microscope. Bar = 50 μm. Merge shows an overlap between green and red fluorescence.

(LECIA TCS SP8) three to four days later. The H$_2$B-mcherry fusion protein was used as a nuclear marker.

AUTHOR-RECOMMENDED INTERNET RESOURCE

IWGSC (International Wheat Genome Sequencing Consortium) database: http://www.wheatgenome.org/Tools-and-Resources/Wheat-Transcript-Resources

LITERATURE CITED

Afzal, A. J., Wood, A. J., and Lightfoot, D. A. 2008. Plant receptor-like serine threonine kinases: Roles in signaling and plant defense. Mol. Plant-Microbe Interact. 21:507-517.

Antolín-Llovera, M., Ried, M. K., Binder, A., and Parniske, M. 2012. Receptor kinase signaling pathways in plant-microbe interactions. Annu. Rev. Phytopathol. 50:451-473.

Bauer, Z., Gómez-Gómez, L., Boller, T., and Felix, G. 2001. Sensitivity of different ecotypes and mutants of *Arabidopsis thaliana* toward the bacterial elicitor flagellin correlates with the presence of receptor-binding sites. J. Biol. Chem. 276:45669-45676.

Bracha-Drori, K., Shichrur, K., Katz, A., Oliva, M., Angelovici, R., Yalovsky, S., and Ohad, N. 2004. Detection of protein-protein interactions in plants using bimolecular fluorescence complementation. Plant J. 40:419-427.

Cantu, D., Yang, B., Ruan, R., Li, K., Menzo, V., Fu, D., Chern, M., Ronald, P. C., and Dubcovsky, J. 2013. Comparative analysis of protein-protein interactions in the defense response of rice and wheat. BMC Genomics 14:166.

Chae, L., Sudat, S., Dudoit, S., Zhu, T., and Luan, S. 2009. Diverse transcriptional programs associated with environmental stress and hormones in the Arabidopsis receptor-like kinase gene family. Mol. Plant 2:84-107.

Chen, X., Coram, T., Huang, X., Wang, M., and Dolezal, A. 2013. Understanding molecular mechanisms of durable and non-durable resistance to stripe rust in wheat using a transcriptomics approach. Curr. Genomics 14:111-126.

Chen, X. M. 2005. Epidemiology and control of stripe rust [*Puccinia striiformis* f. sp *tritici*] on wheat. Can. J. Plant Pathol. 27:314-337.

Chen, X. M. 2007. Challenges and solutions for stripe rust control in the United States. Aust. J. Agric. Res. 58:648-655.

Chen, X. M. 2013. Review article: High-temperature adult-plant resistance, key for sustainable control of stripe rust. Am. J. Plant Sci. 4:608-627.

Chen, X. M., and Line, R. F. 1995. Gene action in wheat cultivars for durable, high-temperature, adult-plant resistance and interaction with race-specific, seedling resistance to *Puccinia striiformis*. Phytopathology 85:567-572.

Cheng, Y., Wang, X., Yao, J., Voegele, R. T., Zhang, Y., Wang, W., Huang, L., and Kang, Z. 2015. Characterization of protein kinase *PsSRPKL*, a novel pathogenicity factor in the wheat stripe rust fungus. Environ. Microbiol. 17:2601-2617.

Chisholm, S. T., Coaker, G., Day, B., and Staskawicz, B. J. 2006. Host-microbe interactions: Shaping the evolution of the plant immune response. Cell 124:803-814.

Dardick, C., Schwessinger, B., and Ronald, P. 2012. Non-arginine-aspartate (non-RD) kinases are associated with innate immune receptors that recognize conserved microbial signatures. Curr. Opin. Plant Biol. 15:358-366.

Darnell, J. E., Jr., Kerr, I. M., and Stark, G. R. 1994. Jak-STAT pathways and transcriptional activation in response to IFNs and other extracellular signaling proteins. Science 264:1415-1421.

Gish, L. A., and Clark, S. E. 2011. The RLK/Pelle family of kinases. Plant J. 66:117-127.

Kim, T. W., and Wang, Z. Y. 2010. Brassinosteroid signal transduction from receptor kinases to transcription factors. Annu. Rev. Plant Biol. 61:681-704.

Kinoshita, A., Betsuyaku, S., Osakabe, Y., Mizuno, S., Nagawa, S., Stahl, Y., Simon, R., Yamaguchi-Shinozaki, K., Fukuda, H., and Sawa, S. 2010. *RPK2* is an essential receptor-like kinase that transmits the CLV3 signal in *Arabidopsis*. Development 137:3911-3920.

Ma, Q., and Shang, H. S. 2000. High-temperature resistance of wheat cultivar Xiaoyan series to wheat stripe rust. Acta Agric. Boreali-Occidentalis Sin. 9:39-42.

Morillo, S. A., and Tax, F. E. 2006. Functional analysis of receptor-like kinases in monocots and dicots. Curr. Opin. Plant Biol. 9:460-469.

Osakabe, Y., Yamaguchi-Shinozaki, K., Shinozaki, K., and Tran, L. S. 2013. Sensing the environment: Key roles of membrane-localized kinases in plant perception and response to abiotic stress. J. Exp. Bot. 64:445-458.

Peng, J. H., Fahima, T., Röder, M. S., Li, Y. C., Dahan, A., Grama, A., Ronin, Y. I., Korol, A. B., and Nevo, E. 1999. Microsatellite tagging of the stripe-rust resistance gene *YrH52* derived from wild emmer wheat, *Triticum dicoccoides*, and suggestive negative crossover interference on chromosome 1B. Theor. Appl. Genet. 98:862-872.

Peng, Y., Bartley, L. E., Chen, X., Dardick, C., Chern, M., Ruan, R., Canlas, P. E., and Ronald, P. C. 2008. *OsWRKY62* is a negative regulator of basal and *Xa21*-mediated defense against *Xanthomonas oryzae* pv. *oryzae* in rice. Mol. Plant 1:446-458.

Pruitt, R. N., Schwessinger, B., Joe, A., Thomas, N., Liu, F., Albert, M., Robinson, M. R., Chan, L. J. G., Luu, D. D., Chen, H., Bahar, O., Daudi, A., De Vleesschauwer, D., Caddell, D., Zhang, W., Zhao, X., Li, X., Heazlewood, J. L., Ruan, D., Majumder, D., Chern, M., Kalbacher, H., Midha, S., Patil, P. B., Sonti, R. V., Petzold, C. J., Liu, C. C., Brodbelt, J. S., Felix, G., and Ronald, P. C. 2015. The rice immune receptor *XA21* recognizes a tyrosine-sulfated protein from a Gram-negative bacterium. Sci. Adv. 1:e1500245.

Rodriguez, M. C. S., Petersen, M., and Mundy, J. 2010. Mitogen-activated protein kinase signaling in plants. Annu. Rev. Plant Biol. 61:621-649.

Schoonbeek, H. J., Wang, H. H., Stefanato, F. L., Craze, M., Bowden, S., Wallington, E., Zipfel, C., and Ridout, C. J. 2015. Arabidopsis *EF-Tu* receptor enhances bacterial disease resistance in transgenic wheat. New Phytol. 206:606-613.

Shen, Q. H., Saijo, Y., Mauch, S., Biskup, C., Bieri, S., Keller, B., Seki, H., Ulker, B., Somssich, I. E., and Schulze-Lefert, P. 2007. Nuclear activity of *MLA* immune receptors links isolate-specific and basal disease-resistance responses. Science 315:1098-1103.

Shiu, S. H., and Bleecker, A. B. 2001. Plant receptor-like kinase gene family: Diversity, function, and signaling. Sci. STKE 2001:re22.

Shpak, E. D., McAbee, J. M., Pillitteri, L. J., and Torii, K. U. 2005. Stomatal patterning and differentiation by synergistic interactions of receptor kinases. Science 309:290-293.

Sui, X. X., Wang, M. N., and Chen, X. M. 2009. Molecular mapping of a stripe rust resistance gene in spring wheat cultivar Zak. Phytopathology 99:1209-1215.

Tang, D., Wang, G., and Zhou, J. M. 2017. Receptor kinases in plant-pathogen interactions: More than pattern recognition. Plant Cell 29:618-637.

Tao, F., Wang, J., Guo, Z., Hu, J., Xu, X., Yang, J., Chen, X., and Hu, X. 2018. Transcriptomic analysis reveal the molecular mechanisms of wheat higher-temperature seedling-plant resistance to *Puccinia striiformis* f. sp. *tritici*. Front. Plant Sci. 9:240.

ten Hove, C. A., Bochdanovits, Z., Jansweijer, V. M., Koning, F. G., Berke, L., Sanchez-Perez, G. F., Scheres, B., and Heidstra, R. 2011. Probing the roles of LRR RLK genes in *Arabidopsis thaliana* roots using a custom T-DNA insertion set. Plant Mol. Biol. 76:69-83.

Wang, J., Tao, F., An, F., Zou, Y., Tian, W., Chen, X., Xu, X., and Hu, X. 2017a. Wheat transcription factor *TaWRKY70* is positively involved in high-temperature seedling plant resistance to *Puccinia striiformis* f. sp. *tritici*. Mol. Plant Pathol. 18:649-661.

Wang, J., Tao, F., Tian, W., Guo, Z., Chen, X., Xu, X., Shang, H., and Hu, X. 2017b. The wheat WRKY transcription factors TaWRKY49 and TaWRKY62 confer differential high-temperature seedling-plant resistance to *Puccinia striiformis* f. sp. *tritici*. PLoS One 12:e0181963.

Xu, X., Chen, C., Fan, B., and Chen, Z. 2006. Physical and functional interactions between pathogen-induced *Arabidopsis* WRKY18, WRKY40, and WRKY60 transcription factors. Plant Cell 18:1310-1326.

Zhang, Z. J., Yang, G. H., Li, G. H., Jin, S. L., and Yang, X. B. 2001. Transgressive segregation, heritability, and number of genes controlling durable resistance to stripe rust in one Chinese and two Italian wheat cultivars. Phytopathology 91:680-686.

Zhang, Z. L., Xie, Z., Zou, X., Casaretto, J., Ho, T. H., and Shen, Q. J. 2004. A rice WRKY gene encodes a transcriptional repressor of the gibberellin signaling pathway in aleurone cells. Plant Physiol. 134:1500-1513.

Zipfel, C., Kunze, G., Chinchilla, D., Caniard, A., Jones, J. D., Boller, T., and Felix, G. 2006. Perception of the bacterial PAMP EF-Tu by the receptor EFR restricts *Agrobacterium*-mediated transformation. Cell 125:749-760.